Journal of Interdisciplinary Mathematics
ISSN: 0972-0502 (Print), ISSN: 2169-012X (Online)
Vol. 29 (2026), No. 1, pp. 95–104
DOI : 10.47974/JIM-2243

Rheological study of hot Bingham fluid inside an oval canal with Laminar peristaltic flow

Hana I. Lafta *
Department of Mathematics
Diyala Education Directorate
Diyala
Iraq

Zainab A. Jaafar †
Department of Mathematics
College of Education -Tuzkhurmatu
Tikrit University
Tikrit
Iraq

Rana G. Ibraheem §
Scientific Research Commission
Baghdad
Iraq

Shuker Khalil ‡
Department of Mathematics
College of Science
University of Basrah
Basrah
Iraq

Abstract

This research article is reported the rheology of peristaltic flow of hot Bingham fluid inside an elliptical channel with sinusoidal moving walls. Convert the dimensional mathematical problem to a dimensionless form when replacing the parameters and using

* *E-mail:* **hanaibra2022@gmail.com (Corresponding Author)**
† *E-mail:* **zainabali611@tu.edu.iq**
§ *E-mail:* **rana.ghazi1103a@sc.uobaghdad.edu.iq**
‡ *E-mail:* **shuker.khalil@uobasrah.edu.iq**

© Taru Publications

the long wavelength approximation. The governing equations were solved analytically to obtain files of velocity, and pressure gradient in addition to solutions for the flowing pressure height. The polynomial used is of the fourth order containing six constants that provide a solution to the velocity and flow function equations by laminar peristaltic transport for a non- Newtonian Bingham fluid. Using the Cartesian coordinate system by employing the ellipse equation in the channel boundary conditions. Showing the behavior of symmetrical axial flow through graphical results in the Mathematica mathematical program. Velocity files have parabolic shapes.

Subject Classification: *Primary 93A30, Secondary 49K15.*

Keywords: *Elliptical duct, Bingham plastic fluid, Cartesian coordinate, Eccentricity of ellipse, Hydraulic diameter.*

1. Introduction

One of the basic topics that have been studied in the dynamics of flow or peristaltic flow between the walls of channels of all kinds is considered a major topic especially in industrial and engineering interests. The peristaltic movement of fluids along the axial directions of the channels due to the abundance of their sinusoidal contractions has contributed widely to enhancing the reality of practical applications of this movement in Newtonian and non -Newtonian fluids. There are many studies and researches that have addressed peristaltic flow in channels with circular sections and other channels with elliptical and rectangular sections [1], [2]. An example of this is a plastic fluid, because it is one of the fluids that require a minimum level of stress to reach the flow state, and because it is basically a non -Newtonian fluid. When it starts moving, this fluid behaves like a Newtonian fluid where the shear stress and shear rate become linear. Accordingly, the shear stress equation is written mathematically in the following formula: $\tau = \tau_y + \text{MpY}$ where τ_y is the yield point $\left(Y_p\right)$ and unit is (pa. s^n), Mp (Mp) represents the plastic viscosity of the fluid and (pv) for the liquid and the unit is maps (cp), (y) represents the shear rate of the fluid. Examples of Bingham plastic fluid are slurries based on water, sewage sludge, most cement mortars, drilling fluids including clay and petroleum derivatives. On the other hand, Bingham fluid does not accurately show the behavior of drilling materials at low shear rates in the ring and at a very high shear rate [3], [4]. Also, some studies in this field [5],[6] are discussed. The governing equations are developed using the approximate transformation to convert these equations are in their non-dimensional forms. Then we have the Partial differential equations for the velocity and energy equations and they were solved according to the boundary conditions set for them on the elliptical section, for the mathematical model when $(\lambda \to \infty)$ with decrease in the Reynolds number and using the Polynomial as a suitable solution method [7, 8].

2. Mathematical Model

We are working on finding mathematical formulas that fit the Non-Newtonian Bingham hot plastic fluid through a duct having elliptical cross-

section. This study using Cartesian coordinates $(\bar{X}, \bar{Y}, \bar{Z})$ with sinusoidally deformed walls and the equations of geometrical model is given as: $\bar{a}(\bar{Z}, \bar{t}) = a_\circ + d\sin(\frac{2\pi}{\lambda}(\bar{Z} - c\bar{t}))$ (1), $\bar{b}(\bar{Z}, \bar{t}) = b_\circ + d\sin(\frac{2\pi}{\lambda}(\bar{Z} - c\bar{t}))$ (2), (a, b, d) and ϕ, respectively symbolize the semi-axes of the cut, the amplitude of the flowing fluid wave and the occlusion. After that, we were able to put the three governing equations in their partial differential and nonlinear form to represent each of the continuity equation, the velocity and the energy equation: $\frac{\partial \bar{\mho}}{\partial \bar{x}} + \frac{\partial \bar{v}}{\partial \bar{y}} + \frac{\partial \bar{w}}{\partial \bar{z}} = 0$ (3) , $\rho\left(\frac{\partial \mho}{\partial \bar{t}} + \bar{\mho}\frac{\partial \bar{\mho}}{\partial \bar{x}} + \bar{V}\frac{\partial \mho}{\partial \bar{y}} + \bar{w}\frac{\partial \bar{\mho}}{\partial \bar{z}}\right) = -\frac{\partial \bar{P}}{\partial \bar{x}} + \frac{\partial \bar{S}_{\bar{x}\bar{x}}}{\partial \bar{x}} + \frac{\partial \bar{S}_{\bar{y}\bar{x}}}{\partial \bar{y}} + \frac{\partial \bar{S}_{\bar{z}\bar{x}}}{\partial \bar{z}}$ (4), $\rho\left(\frac{\partial \bar{v}}{\partial \bar{t}} + \bar{\mho}\frac{\partial \bar{v}}{\partial \bar{x}} + \bar{V}\frac{\partial \bar{v}}{\partial \bar{y}} + \bar{w}\frac{\partial \bar{v}}{\partial \bar{z}}\right) = -\frac{\partial \bar{P}}{\partial \bar{y}} + \frac{\partial \bar{S}_{\bar{x}\bar{y}}}{\partial \bar{x}} + \frac{\partial \bar{S}_{\bar{y}\bar{y}}}{\partial \bar{y}} + \frac{\partial \bar{S}_{\bar{y}\bar{z}}}{\partial \bar{z}}$ (5),

$$\rho\left(\frac{\partial \bar{w}}{\partial \bar{t}} + \bar{\mho}\frac{\partial \bar{w}}{\partial \bar{x}} + \bar{V}\frac{\partial \bar{w}}{\partial \bar{y}} + \bar{w}\frac{\partial \bar{w}}{\partial \bar{z}}\right) = -\frac{\partial \bar{P}}{\partial \bar{z}} + \frac{\partial \bar{S}_{\bar{x}\bar{z}}}{\partial \bar{x}} + \frac{\partial \bar{S}_{\bar{y}\bar{z}}}{\partial \bar{y}} + \frac{\partial \bar{S}_{\bar{z}\bar{z}}}{\partial \bar{z}} - \sigma B_\circ^2 \bar{w}$$

(6),

$$\rho c_p\left(\frac{\partial \bar{T}}{\partial \bar{t}} + \bar{\mho}\frac{\partial \bar{T}}{\partial \bar{x}} + \bar{V}\frac{\partial \bar{T}}{\partial \bar{y}} + \bar{w}\frac{\partial \bar{T}}{\partial \bar{z}}\right) = K\left(\frac{\partial^2 \bar{T}}{\partial \bar{X}^2} + \frac{\partial^2 \bar{T}}{\partial \bar{y}^2} + \frac{\partial^2 \bar{T}}{\partial \bar{z}^2}\right) + \bar{S}_{\bar{x}\bar{x}}\frac{\partial \mho}{\partial \bar{x}} + \bar{S}_{\bar{x}\bar{y}}\frac{\partial \mho}{\partial \bar{y}} + \bar{S}_{\bar{x}\bar{z}}\frac{\partial \mho}{\partial \bar{z}} + \bar{S}_{\bar{y}\bar{x}}\frac{\partial \bar{v}}{\partial \bar{x}} + \bar{S}_{\bar{y}\bar{y}}\frac{\partial \mho}{\partial \bar{y}} + \bar{S}_{\bar{y}\bar{z}}\frac{\partial \bar{v}}{\partial \bar{z}} + \bar{S}_{\bar{z}\bar{x}}\frac{\partial \mho}{\partial \bar{z}} + \bar{S}_{\bar{y}\bar{x}}\frac{\partial \bar{w}}{\partial \bar{x}} + \bar{S}_{\bar{z}\bar{y}}\frac{\partial \bar{w}}{\partial \bar{y}} + \bar{S}_{\bar{z}\bar{z}}\frac{\partial \bar{w}}{\partial \bar{z}}$$

(7), The conditions placed on the walls of the channel are: $\bar{w} = 0, \bar{T} = \bar{T}_w \; for \; \frac{\bar{x}^2}{\bar{a}^2} + \frac{\bar{y}^2}{\bar{b}^2} = 1$ (8) . Where the velocity components $(\bar{U}, \bar{V}, \bar{W})$ and the extra stress tensor $\bar{S}_{ij}$,(i,j=1,2,3) are available, as well as the thermal conductivity (k) in the equations of the problem. The Bingham fluid stress tensor is defined as $\sigma^* = -PI + \bar{S}$ (9). Where $\bar{S} = 2M_P D + 2\tau_\circ \bar{D}$…. (10). Here ($\tau_\circ$) is the product stress and (D), the tensor while ($\bar{D}$) the rate of deformation defined as: $\bar{D} = \frac{D}{\sqrt{2traD^2}}$, $D = \frac{1}{2}(\nabla\bar{V} + (\nabla\bar{V})^{\mathrm{T}})$ (11). The transformation from laboratory frame $(\bar{X}, \bar{Y}, \bar{Z})$ to wave frame $(\bar{X}, \bar{Y}, \bar{Z})$ are given as: $\bar{x} = \bar{X}, \bar{u} = \bar{U}, \bar{y} = \bar{Y}, \bar{v} = \bar{V}, \bar{p} = \bar{P}, \bar{w} = \bar{W} - C, \bar{z} = \bar{Z} - c\bar{t}$ (12). Dimensionless analysis of momentum equations are given by: $X = \frac{\bar{X}}{D_h}, y = \frac{\bar{y}}{D_h}, Z = \frac{\bar{Z}}{\lambda}, t = \frac{ct}{\lambda}, \emptyset = \frac{d}{b_\circ}, w = \frac{\bar{W}}{C}, \theta = \frac{\bar{T} - T_w}{\bar{T}_b - \bar{T}_w}, P = \frac{D_h^2 \bar{P}}{M\lambda c}, S = \frac{b_\circ}{a_\circ}, U = \frac{\lambda \bar{u}}{D_h C}, V = \frac{\lambda \bar{v}}{D_h C}, B_r = \frac{MC^2}{K(\bar{T}_b - \bar{T}_w)}, S_{ij} = \frac{D_h \bar{S}_{ij}}{CM_P}, a = \frac{\bar{a}}{D_h}, b = \frac{\bar{b}}{D_h}, h_1 = \frac{\bar{H}_1}{D_h}, h_2 = \frac{\bar{H}_2}{D_h}, B_n = \frac{\tau_\circ D_h}{CM_P}, M^2 = \frac{D_h^2 B_\circ^2 \sigma}{M_P}, R_e = \frac{\rho D_h C}{M_P}, D_h = \frac{\pi b_\circ}{E(e)}$ (13), $D_h = \frac{4\bar{A}}{\bar{\ell}} = \frac{\pi b_\circ}{E(e)}$ (14). Note that $D_h,\ A \; and \; \bar{\ell}$, it symbolizes the hydraulic diameter, the cross -sectional area and perimeter of duct. Moreover $e = \sqrt{1 - \delta^2}$, and $E(e) = \int_\circ^{\frac{\pi}{2}} \sqrt{1 - e^2 sin^2 \propto} \, d \propto$ (15). Applying lubrication approximation $(\lambda \to \infty)$ into equations 3- 6 to obtain non-dimensional governing equations as: $\frac{\partial p}{\partial x} = 0$ (16), $\frac{\partial p}{\partial y} = 0$ (17), $\frac{\partial p}{\partial z} = \left(1 + \frac{B_n}{\sqrt{\left(\frac{\partial w}{\partial x}\right)^2 + \left(\frac{\partial w}{\partial y}\right)^2}}\right)\left(\frac{\partial^2 w}{\partial x^2} + \frac{\partial^2 w}{\partial y^2}\right) - M^2 R^{/}(w + 1)$ (18), $O = \frac{\partial^2 \theta}{\partial x^2} + \frac{\partial^2 \theta}{\partial y^2} +$

$\frac{B_T\pi^2 b_o^2}{(E(e))^2}\left(1+\frac{B_n}{\sqrt{\left(\frac{\partial w}{\partial x}\right)^2+\left(\frac{\partial w}{\partial y}\right)^2}}\right)\left(\left(\frac{\partial w}{\partial x}\right)^2+\left(\frac{\partial w}{\partial y}\right)^2\right)$ (19). With dimensional of boundary conditions in the wave frames. $w=-1$ for $\frac{\bar{x}^2}{\bar{a}^2}+\frac{\bar{y}^2}{\bar{b}^2}=1, \theta = 0$ for $\frac{\bar{x}^2}{\bar{a}^2}+\frac{\bar{y}^2}{\bar{b}^2}=1$ (20), $a=\frac{E(e)}{\pi}\left(\frac{1}{S}+\emptyset\sin 2\pi z\right)$, $b=\frac{E(e)}{\pi}(1+\emptyset\sin 2\pi z)$ (21).

3. Exact Solution

We can express and formulate the velocity in this polynomial solution method $w(x,y)=C_1x^4+C_2y^4+C_3x^2y^2+C_4x^2+C_5y^2+C_6$ (22).

It is best to use the equation (22) for a purpose to use in motion equation and the boundary conditions, by substituting eq.(22) in eq.(18) and making compare of $x^2, y^2, x^\circ, y^\circ$ on both sides of this equation, we get three equations. $B_nC_3+6B_nC_2-M^2RC_5^2=0$ (i), $6B_nC_1+B_nC_3-M^2RC_4^2=o$ (ii), $2C_4+2C_5-M^2R(1+C_6)=\frac{\partial p}{\partial z}$ (iii). On the other hand, we find another three equations by applying (22) in equation (20), and we have the coefficients of X^Δ, X^2, X° given in the following form: $C_1a^4+C_2b^4-C_3a^2b^2=o$ (iv), $2C_2b^4-C_3a^2b^2-C_4a^2+C_4b^2=o$ (v), $C_2b^4+C_5b^2+C_6=-1$ (vi). When we solve these equations (i) – (vi) and find the values of six constant, we get the exact solution of velocity as: $w(x,y)=(\mathrm{Bn}(-9a^{26}\mathrm{Bn}^2M^{10}R^5(2\mathrm{Bn}+b^2M^2R(\frac{\partial p}{\partial z}+b^4M^2R))+3a^{24}\mathrm{Bn}^2M^8 \quad R^4(\mathrm{Bn}(60-72b^2M^2R)-b^2M^2R(-30+19b^2M^2R)$ (23). So the dimensionless velocity at the middle of the channel becomes: $W_c=(\mathrm{Bn}(-9a^{26}\mathrm{Bn}^2M^{10}R^5\left(2\mathrm{Bn}+b^2M^2R\left(\frac{\partial p}{\partial z}+b^4M^2R\right)\right)+3a^{24}\mathrm{Bn}^2M^8R^4\left(\mathrm{Bn}(60-72b^2M^2R)-b^2M^2R(-30+19b^2M^2R)\right)$ (24). The exact solution of the volumetric flux is computed by integration velocity term over the elliptical domain: $q(z)=((\mathrm{Bn}(-9a^{26}\mathrm{Bn}^2M^{10}R^5\left(2\mathrm{Bn}+b^2M^2R\left(\frac{\partial p}{\partial z}+b^4M^2R\right)\right)+3a^{24}\mathrm{Bn}^2M^8R^4(\mathrm{Bn}(60-72b^2M^2R)-b^2M^2R(-30+19b^2M^2R)(\frac{\partial p}{\partial z}+b^4M^2R))+576b^{10}\mathrm{Bn}^2(-6b^6\mathrm{Bn}+\sqrt{(36(a^6+7a^4b^2+7a^2b^4+b^6)^2\mathrm{Bn}^2}$ (25).

4. Discussion of the Result

We discuss the velocity profile and stream line function in 2- dimensional and obtained from the polynomial.

4.1 *Velocity Function*

Figures 1-5 supply all in formations for the graphical outcomes of fluids velocity, since the solution is close to infinity its Newtonian behavior will fail, so we don't need to discuss it here. Figures 1 and 4 explain decreases observed

in velocity as increment of the value of the volumetric flux rate for increasing the parameter a and B_n in the core of duct and walls, we can get close the walls of the ellipse duct. Figures 2, 3 and 5 depict the 2-dimensional velocity graphs for increasing in the velocity function is visible with increment values of M, R and b, the flux profile investigate elevation, volume in the centric domain of the duct, but it shows an opposite behavior approach the wall boundaries with a rise value of M, b and R parameters. This graphs interpret the velocity graphs that flux behavior is axially symmetric and parabolic.

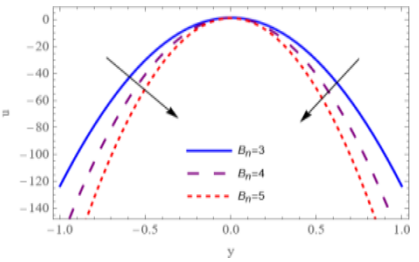

Figure 1
Velocity variation for different (B_n) values when $M = 3, R = 6, a = 0.1, b = 0.1, x = 1$

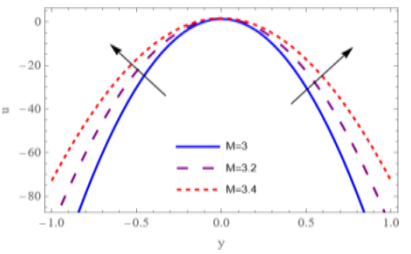

Figure 2
Velocity variation for different (M) values when Bn $= 3, R = 6, a = 0.1, b = 0.1, x = 1$

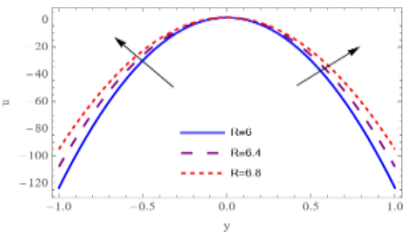

Figure 3
Velocity variation for different (R) values when Bn $= 3, M = 3, a = 0.1, b = 0.1, x = 1$

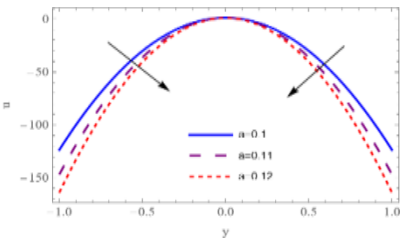

Figure 4
Velocity variation for different (a) values when Bn $= 3, M = 3, R = 6, b = 0.1, x = 1$

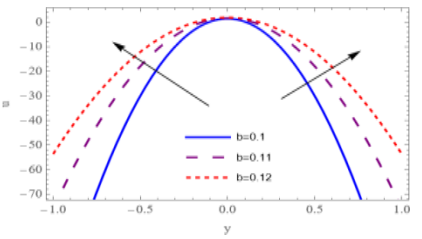

Figure 5
Velocity variation for different (b) values when Bn $= 3, M = 3, R = 6, a = 0.1, x = 1$

4.1 *Streamlines Function*

Figures 6-10 reveals the streamlines analysis of Bingham fluid during an elliptical cross section canal under the peristalsis flux and generation of trapping bolus for various values of flux. Figure 6 recorded the increase in B_n cause the boluses to separate from each other and come closer to the walls. The ability of parameter M to increase directly affects the reduction in the number of boluses, in addition to the distance of the bolus from each other towards the walls, see figure 7. Figure 8, depicts increasing in R ensures an increase of number and size of boluses, especially when approaching the center of the duct. From figure 9, by increasing the value of a, we notice a decrease in the number and size of boluses in the central part of duct and their expansion at the upper wall. The increase in b contributed significantly to the increase in the number and size of boluses in the middle of the duct and its disappearance at the upper wall.

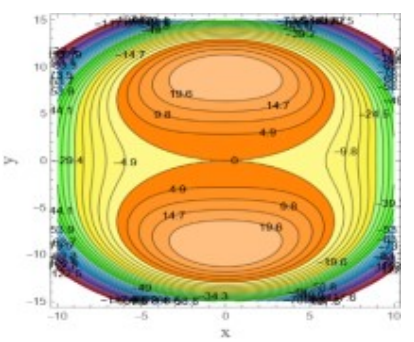

Figure (6-A): For (A) $B_n = 3$

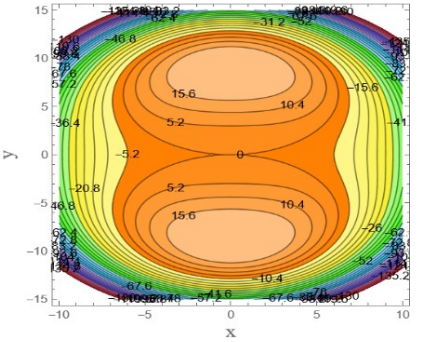

Figure (6-B): For (B) $B_n = 3.5$

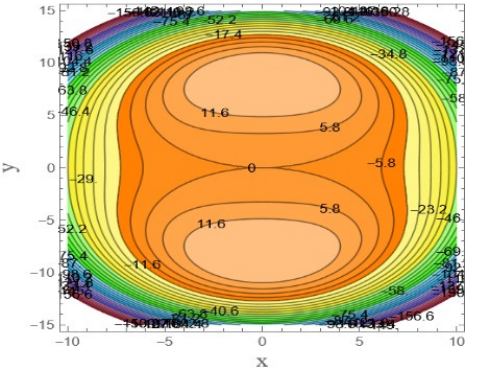

Figure (6-C): For (C) $B_n = 4$.

Figure 6
Distribution of streamline for (A) $B_n = 3$, (B) $B_n = 3.5$, (C) $B_n = 4$.

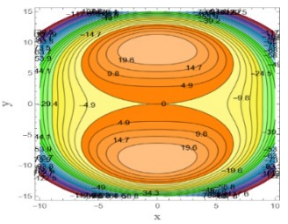

Figure (7-A): For (A) M = 3

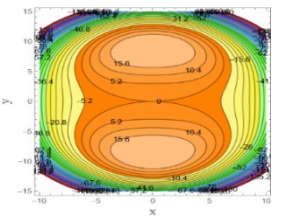

Figure (7-B): For (B) M = 3.03

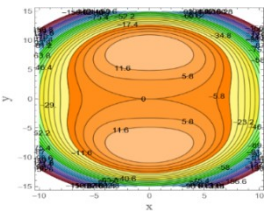

Figure (7-C): For (C) M = 3.07

Figure 7

Distribution of streamline for(A) M = 3,(B) M = 3.03, (C)M = 3.07

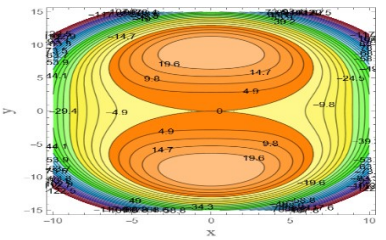

Figure (8-A): For (A) R = 6

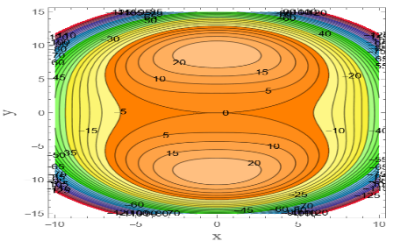

Figure (8-B): For (B) R = 6

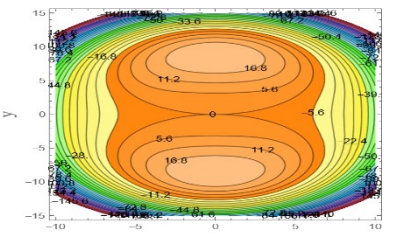

Figure (8-C): For (C) R = 6.2

Figure 8

Distribution of streamline for (A)R=6, (B)R=6.1, (C)R=6.2.

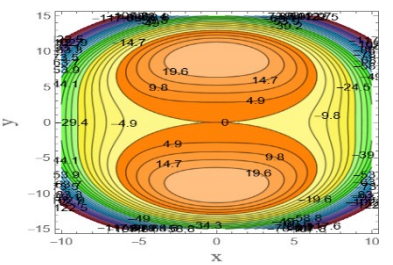

Figure (9-A): For (A) a = 0.1

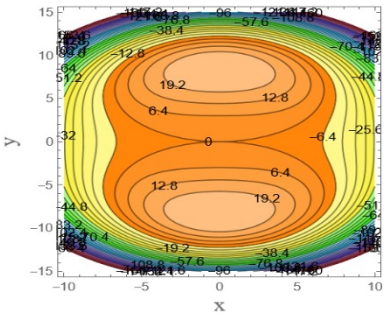

Figure (9-B): For (B) $a = 0.11$

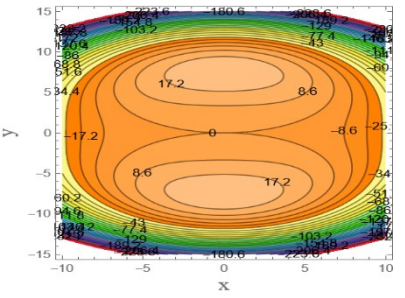

Figure (9-C): For (C) $a = 0.12$

Figure 9

Distribution of streamline for (A)a=0.1, (B)a=0.11, (C)a=0.12.

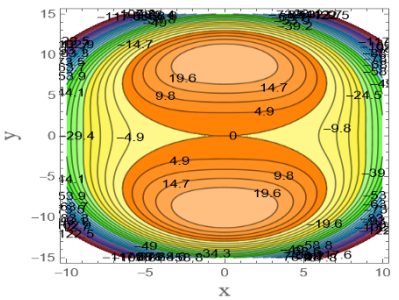

Figure (10-A): For (A) $b = 0.1$

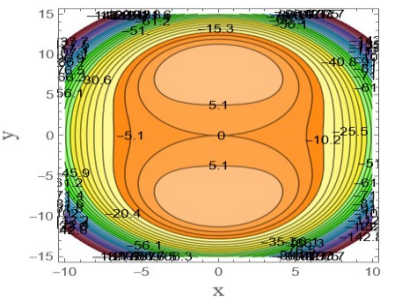

Figure (10-B): For (B) $b = 0.11$

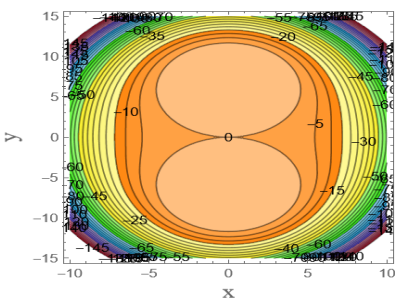

Figure (10-C): For (C)$b = 0.12$

Figure 10

Distribution of streamline for (A)b=0.1, (B)b=0.11, (C)b=0.12.

5. Discussion and Conclusion

This article reports the peristaltic movement of a heated Bingham fluid inside an elliptical duct possessing sinusoidal moving walls. To obtain an exact solution, we have employed the newness polynomial of order four, having six constants, to solve the velocity equation exactly for Bingham fluid flow during an elliptic region. Then we have deduced the main points listed below:

1. Velocity function has a parabolic shape, increasing values B_n and a contributes to the decrease in velocity despite small values near the walls of the velocity function.
2. The increase in the values M, R, and b mainly causes the sudden increase in the velocity at the duct walls and core.
3. The increment behavior of velocity at the centric attractions to a reducing one close to the duct walls.
4. The direct effect of the flow is apparent when the values of R and b increase; the number and size of boluses increase.
5. Decrease in the number of boluses and their small size when the values of M and a rise and their gradual disappearance at the walls.
6. Bingham parameter has a positive effect on the velocity profile, as the velocity improved significantly at the walls of duct. Conversely, when the values of B_n increased it led to the separation of the boluses and their distancing from each other, and then their strong convergence at the walls of the duct.

References

[1] Bingham, E. C., Fluidity and plasticity. McGraw-Hill Book Company, Incorporated (1922).

[2] Z. A. Jaafar, L. Z. Hummady, and M. H. Thawi, "Effects of Rotation and Inclined Magnetic Field on Walters' B Fluid in a Porous Medium using perturbation method or technique.," *Iraqi J Sci* (2024).

[3] P. S. Sekhar, V. S. Sajja, and V. V. R. Murthy, "Bingham plastic fluid flow between two parallel plates with temperature effect," *Int J Innov Technol Explor Eng*, pp. 307–309 (2019).

[4] A. P. A. Lucky and F. A. Johnson, "Modification of Bingham plastic rheological model for better rheological characterization of synthetic based drilling mud," *J Eng Appl Sci,* vol. 13, no. 10, pp. 3573–3581 (2018).

[5] Z. A. Jaafar, H. I. Lafta, Numerical computation for effect of inclined magnetic field on hyperbolic tangent peristalsis flow suspension in a porous medium, *Journal For Basic Sciences,* vol. 14, no. 22, pp. 333–353 (2024).

[6] T. H. Jasim, H. I. Lafta, S. M. Abdullah, Some types of separation axioms for (k,m)-generalized Fuzzy W-(resp., Fuzzy w*)-closed sets n dFts., *Journal of Interdisciplinary Mathematics*, vol. 24, no.7, pp. 1787-1798 (2021).

[7] S. M. Noori, A. G. Ahmad, S. Khalil, The decision-making process in learners' failure using fuzzy scale, *Journal of Interdisciplinary Mathematics*, vol. 26 no. 7, pp. 1533–1540 (2023).

[8] S. Khalil, "Decision Making Using New Category of Similarity Measures and Study Their Applications in Medical Diagnosis Problems," *Afrika Matematika,* vol. 32, pp. 865–878 (2021). doi: 10.1007/s13370-020-00866-2.

Received March, 2025